HHS Public Access

Author manuscript

Dev Biol. Author manuscript; available in PMC 2018 December 01.

Published in final edited form as:

Dev Biol. 2017 December 01; 432(1): 86–97. doi:10.1016/j.ydbio.2017.08.036.

Optimization of CRISPR-Cas9 genome editing for loss-of-function in the early chick embryo

Shashank Gandhi, **Michael L. Piacentino**, **Felipe M. Vieceli**, and **Marianne E. Bronner***

Division of Biology and Biological Engineering, California Institute of Technology, Pasadena, CA 91125

Abstract

The advent of CRISPR/Cas9 has made genome editing possible in virtually any organism, including those not previously amenable to genetic manipulations. Here, we present an optimization of CRISPR/Cas9 for application to early avian embryos with improved efficiency via a three-fold strategy. First, we employed Cas9 protein flanked with two nuclear localization signal sequences for improved nuclear localization. Second, we used a modified guide RNA (gRNA) scaffold that obviates premature termination of transcription and unstable Cas9-gRNA interactions. Third, we used a chick-specific U6 promoter that yields 4-fold higher gRNA expression than the previously utilized human U6. For rapid screening of gRNAs for in vivo applications, we also generated a chicken fibroblast cell line that constitutively expresses Cas9. As proof of principle, we performed electroporation-based loss-of-function studies in the early chick embryo to knock out Pax7 and Sox10, key transcription factors with known functions in neural crest development. The results show that CRISPR/Cas9-mediated deletion causes loss of their respective proteins and transcripts, as well as predicted downstream targets. Taken together, the results reveal the utility of this optimized CRISPR/Cas9 method for targeted gene knockout in chicken embryos in a manner that is reproducible, robust and specific.

Keywords

CRISPR/Cas9; chick embryos; gRNA; neural crest; knockout

Introduction

Chick embryos have long been used as a model organism to address important questions in developmental biology due to their accessibility to transplantation, surgical ablations, and

*Corresponding author.

Author Contributions

S.G. and M.E.B. conceived this study. S.G., M.L.P., F.M.V., and M.E.B. designed the experiments. S.G., M.L.P. and F.M.V performed the experiments and analyzed the results. S.G., M.L.P. and M.E.B. wrote the manuscript.

Conflicts of Interest

The authors declare no competing or financial interests.

other genetic perturbations. This has allowed researchers to regulate gene expression in a spatiotemporally controlled manner at diverse stages of development (Darnell and Schoenwolf, 2000; Streit et al., 2013). Traditionally, loss-of-function experiments have utilized anti-sense morpholinos (Corey and Abrams, 2001), dominant-negative constructs or shRNAs (Sauka-Spengler and Barembaum, 2008). However, these techniques are transient, becoming diluted by cell proliferation during development, and there have been increasing concerns regarding possible lack of specificity due to either off-target effects or reagent toxicity (Eisen and Smith, 2008; Gerety and Wilkinson, 2011; Kok et al., 2015; Schulte-Merker and Stainier, 2014).

One alternative to these approaches is CRISPR/Cas9 (Clustered Regularly Interspaced Short Palindromic Repeats/CRISPR-Associated protein 9), a revolutionary technology that has enabled efficient knockout of target genes across a wide range of model organisms (Cong et al., 2013; Dickinson et al., 2013; Gagnon et al., 2014; Ren et al., 2014; Stolfi et al., 2014). CRISPR/Cas9 involves the formation of a complex between guide RNA (gRNA) and Cas9, an endonuclease enzyme derived from *Streptococcus pyogenes*, which then binds to specific targets in the genome. Once bound to genomic DNA, this complex introduces double-stranded breaks that are imperfectly repaired by Non-Homologous End Joining repair enzymes, often leading to a frame-shift insertion or deletion, and subsequent truncation and/or degradation of the target transcript (Jinek et al., 2012; Qi et al., 2013; Sternberg et al., 2014). Specificity is achieved through Watson-Crick base pairing between the protospacer domain of the gRNA and the target locus in the genome, together with recognition of a Protospacer Adjacent Motif (PAM) by Cas9. Not only does CRISPR/Cas9 offer high spatiotemporal specificity (Stolfi et al., 2014), but it also enables investigation of the roles of non-coding genetic elements such as enhancers and insulators in regulating gene expression during development (Diao et al., 2016; Han et al., 2014; Korkmaz et al., 2016; Lopes et al., 2016; Thakore et al., 2015).

In spite of all its advantages, the CRISPR/Cas9 system has not been fully optimized for application in chick embryos. Early attempts at implementation in avian embryos employed a tetracycline-inducible Cas9 system to perform gene editing of Pax7 using Tol-2 mediated integration at stages after neural tube closure (Véron et al., 2015). While useful, this approach functioned at low efficiency, particularly at early developmental stages (Bai et al., 2016; Oishi et al., 2016; Véron et al., 2015). Since then, several studies performed in other model systems have reported optimizations of individual CRISPR/Cas9 components, improving our understanding of this gene-editing technology (Chen et al., 2013; Doench et al., 2016; Gandhi et al., 2017; Port et al., 2014; Ren et al., 2014).

To extend the usefulness of this technique to the early chick embryo, we have adapted an optimized CRISPR/Cas9 system for efficient genome editing by implementing three modifications. First, we used a previously characterized Cas9 protein flanked with two nuclear localization sequences (NLS) for enhanced compartmentalization in the nucleus (Chen et al., 2013; Stolfi et al., 2014). Second, we used a modified gRNA “F+E” scaffold that has been shown to resolve issues including premature termination of RNA Polymerase-III-mediated transcription of the gRNA cassette and unstable interaction between Cas9 protein and transcribed gRNA (Chen et al., 2013; Orioli et al., 2011). Third, we improved

gRNA expression by using a chick-specific U6 promoter that outperforms a human U6 promoter in chick embryos (Cong et al., 2013; Kudo and Sutou, 2005; Wise et al., 2007).

In the present study, we demonstrate the efficiency of this improved CRISPR/Cas9 system by performing functional testing in the avian neural crest. The neural crest is a multipotent cell population that originates at the neural plate border, then migrates extensively throughout the embryo to give rise to numerous cell types (Le Douarin and Kalcheim, 1982; Green et al., 2015; Simões-Costa and Bronner, 2015). We test the ability of our optimized CRISPR/Cas9 system to knock out key transcription factors in the neural crest, including the neural plate border specifier Pax7 (Basch et al., 2006), and the neural crest specifier, Sox10 (Betancur et al., 2010; Carney et al., 2006), among others. The results show that our CRISPR/Cas9 system is robust and reproducible as a means for knocking out genes of interest in chicken embryos.

Results and Discussion

Here, we present a strategy using optimized CRISPR/Cas9 components to enable efficient knockouts at early developmental stages, starting with the transcription factor Pax7 and extending our approach to other genes of known importance in chick neural crest development.

Optimizing CRISPR/Cas9 components for application in chick embryos

As a first step, we cloned a previously published human codon-optimized *spCas9* (Qi et al., 2013) flanked with an NLS sequence on both the N and C-terminus under the regulation of the chicken beta-actin promoter (CAGG) (Alexopoulou et al., 2008) to ensure optimal nuclear localization of Cas9 protein *in vivo* (Figure 1A). It was previously shown that two NLS sequences are necessary for proper nuclear localization of Cas9 protein (Chen et al., 2013). Co-electroporation of Cas9 (*CAGG>nls-Cas9-nls*) with *CAGG>H2B-RFP* and a control gRNA (*U6.3>Control.gRNA.f+e*), followed by immunostaining for Cas9 protein demonstrated effective nuclear localization in transfected cells (Figure 1B–D). Second, we cloned all protospacer sequences targeting genes of interest in a previously modified gRNA 'F+E' scaffold (Figure 1E) that contains a 'flipped' (F) Adenine-Uracil pair downstream of the protospacer domain and an 'extended' (E) Cas9 stem handle (Chen et al., 2013). These modifications were shown to improve RNA polymerase III-mediated gRNA transcription by minimizing the possibility of premature termination of transcription, as well as stabilize the interaction between Cas9 protein and the transcribed gRNA, respectively (Chen et al., 2013; Stolfi et al., 2014). Third, we tested different RNA Polymerase III-mediated promoters for their ability to drive gRNA expression in transfected cells *in vivo*. Although most CRISPR knockout experiments performed in mammalian systems have used a human U6 promoter to govern gRNA expression (Jinek et al., 2013; Mali et al., 2013; Wang et al., 2014), species-specific U6 promoters have been used in non-mammalian model organisms such as zebrafish, Ciona, and Drosophila (Ablain et al., 2015; Nishiyama and Fujiwara, 2008; Port et al., 2014). To that effect, we directly compared gRNA expression levels mediated by the standard human U6 (hU6) promoter with a chicken U6 (cU6.3) promoter.

To this end, we electroporated the right side of gastrulating chick embryos at Hamburger Hamilton stage 4 (HH4) (V. Hamburger, 1951) with different *U6-variant>bCat.gRNA.f+e.NoTermGFP* constructs (Figure 1F; see Materials and Methods for details), and allowed embryos to develop until stage HH9-10. A reporter (*CAGG>H2B-RFP*) was co-electroporated to normalize electroporation variability between embryos. Using *in situ* hybridization against GFP, we observed increased gRNA transcription with the chicken U6.3 promoter variant compared with the hU6 promoter (Figure 1G–H). After isolating RNA and reverse-transcribing cDNA from three biological replicates electroporated with the two variants, we performed quantitative RT-PCR (qRT-PCR) using primers specific to GFP. The results confirmed our *in situ* hybridization analysis, showing that the chicken-specific U6.3 promoter resulted in a 4-fold increase in gRNA transcription compared to a human U6 promoter used in previous studies (Figure 1I). The chicken U6.3 promoter variant also outperformed an additional chick U6 promoter (data not shown), demonstrating that intra-species variability should be considered when selecting promoters to drive expression of small RNA molecules. Taken together, our results identify chicken-specific U6.3 promoter as an improvement over previously used human U6 promoters for gRNA transcription, and highlight the importance of U6 promoter selection for subsequent loss-of-function studies.

In addition to improving the U6 promoter for delivery of gRNA, we incorporated a screening step into our gRNA design strategy to help eliminate the possibility of off-target effects. Multiple groups have previously highlighted design principles that correlate directly with the activity of the gRNA *in vivo* (Cho et al., 2014; Gandhi et al., 2017; Tsai et al., 2015). To simplify our gRNA design, we considered these principles and employed the MIT CRISPR program (http://crispr.mit.edu) for initial target site selection. When presented with multiple protospacer sequences, those with high scoring alignments outside the desired locus were discarded. As such, all gRNAs used for functional analysis in this study were designed to avoid off-target gRNA sites, thereby minimizing non-specific effects.

CRISPR/Cas9-mediated knockout of key neural crest genes

To establish proof of principle, we first used our optimized CRISPR system to target the transcription factor Pax7 in chick embryos. Pax7 is one of the earliest markers of the neural plate border, and its loss using a translation-blocking morpholino results in a significant decrease in neural crest markers such as *Snai2*, *Sox9*, and *FoxD3* (Basch et al., 2006; Labosky and Kaestner, 1998; Simões-Costa and Bronner, 2015; Simões-Costa et al., 2012). We designed a gRNA targeting the splice acceptor site of the second exon of Pax7 (Figure 2A) and expressed it under the regulation of the optimized chicken U6.3 promoter (*U6.3>Pax7.1.gRNAf+e*). To confirm CRISPR-mediated genomic editing at the desired locus, we co-electroporated *U6.3>Pax7.1.gRNAf+e* along with *CAGG>nls-Cas9-nls* and *CAGG>H2B-RFP* bilaterally, and harvested embryos at stage HH10. Embryos were dissociated to isolate RFP^+ cells by flow cytometry, which were then used to prepare genomic DNA for genotyping. The target locus was PCR-amplified and sequenced to identify CRISPR-induced mutations. As expected, a range of different insertion (red) and deletion (gray) mutations were identified in the gRNA target sequence (Figure 2B), demonstrating that the Cas9 protein used in this study can induce targeted genomic mutations. We next co-electroporated the Pax7-targeting gRNA (*U6.3>Pax7.1.gRNAf+e*)

along with *CAGG>nls-Cas9-nls* and *CAGG>H2B-RFP* on the right side of gastrulating stage HH4 embryos, and then cultured these until developmental stage HH9^{+} (Figure 2C). The left side was electroporated with a control gRNA that has no recognition sites in the chick genome (*U6.3>Control.gRNAf+e*) and served as an internal control. Immunostaining using a Pax7 antibody revealed downregulation of Pax7 protein level on the side electroporated with *Pax7.1* gRNA compared to the control side (Figure 2D), consistent with the anticipated splicing errors and/or frame shifts following Cas9-induced mutations. When overlaying RFP and Pax7 channels, we observed that all cells that were successfully transfected with the H2B-RFP plasmid showed no detectable Pax7 protein compared to the control side, where transfected neural crest cells were double-positive for RFP and Pax7 (Figure 2E, E′, E″). This was particularly interesting because Pax7 is expressed in the neural plate border as early as stage HH4+ (Basch et al., 2006; Roellig et al., 2017). Given that several hours after electroporation are required for the production of Cas9 protein after electroporation (Stolfi et al., 2014), this suggests that the half-life of Pax7 protein is short enough for our CRISPR/Cas9 system to cause loss of Pax7 protein expression within 14 hours. To confirm that loss of Pax7 would manifest itself in a loss of neural crest migration phenotype, we co-immunostained stage HH10 embryos for HNK1, a surface antigen that has traditionally been used as a marker for migratory neural crest cells (Basch et al., 2006). As expected, we saw a strong loss of HNK1 expression on the Pax7 knock out side of the embryo compared to the control side (Figure 2F), suggesting that loss of Pax7 protein resulted in the failure of neural crest specification and ultimately, migration. In other embryos, we co-electroporated *CAGG>nls-Cas9-nls* and *U6.3>Pax7.1.gRNAf+e* unilaterally on the right side at stage HH4, and allowed the embryos to develop until stage HH9. Transverse sections through a representative embryo revealed an almost complete loss of Pax7 expression in the dorsal neural tube (Figure 2G–2G″). Looking closer at this region, we saw that the number of cells, as assessed by 4,6–diamidino-2-phenylindole (DAPI) staining, appeared unchanged (Figure 2G‴). This suggests that the loss in Pax7 expression was a result of CRISPR/Cas9-mediated modification of the *Pax7* locus, and that the concentration of plasmids electroporated in the embryo did not result in cellular toxicity.

Once we verified efficient reduction in protein levels, we asked whether this effect reflects the presence of fewer transcripts of target genes following CRISPR/Cas9-mediated mutations. To test this, we designed a gRNA targeting the start codon of Sox10 (Figure 3A), a transcription factor expressed in the migrating neural crest (Figure 3C) that plays a critical role in the migratory neural crest gene regulatory network (Betancur et al., 2010; Carney et al., 2006; Ghislain et al., 2003). We began by co-electroporating *CAGG>nls-Cas9-nls, U6.3>Sox10.1.gRNAf+e*, and *CAGG>H2B-RFP* bilaterally in stage HH4 embryos, and genotyping RFP^{+} cells sorted by flow cytometry as described above for the Pax7 locus. Similar to Pax7, we identified several mutations surrounding the Sox10 target sequence (Figure 3B). We co-electroporated *CAGG>nls-Cas9-nls, U6.3>Sox10.1.gRNAf+e*, and a reporter *CAGG>H2B-RFP* on the right side of a stage HH4 embryo. The left side was electroporated with *U6.3>Control.gRNAf+e* and served as an internal control. Embryos were cultured *ex ovo* until stage HH9-10, then processed for *in situ* hybridization. The results reveal a substantial decrease in Sox10 transcript levels on the side electroporated with the *Sox10.1* gRNA (Figure 3D, E), both in the neural crest and in the otic placode (Figure

3E′) (Betancur et al., 2011). The loss of transcripts detected by in situ hybridization is consistent with the degradation of mutant transcripts by nonsense-mediated decay (Losson and Lacroute, 1979). To confirm that the effect on Sox10 transcripts is reflected at the Sox10 protein level, we immunostained for Sox10 protein in embryos electroporated using the same strategy. We observed a nearly complete loss of Sox10 in the right side of the embryo following *Sox10.1* gRNA electroporation (Figure 3F, F′). Similarly, knock-out of Pax7 caused a near complete loss of Pax7 transcripts (Figure 4A). Taken together, these results show that our CRISPR/Cas9 system is highly robust at causing loss of function of target genes.

To extend this system to other genes implicated in neural and neural crest development, we designed gRNAs against Sox2 and performed electroporations similar to those described above. The result demonstrates efficient loss of Sox2 protein on the electroporated side of the same embryo compared to the control side (Supplemental Figure 1).

Establishing epistatic relationships using CRISPR/Cas9

The ability to knock out genes of interest is particularly important when constructing gene regulatory networks underlying developmental events. To demonstrate that CRISPR/Cas9 can be used to interrogate regulatory relationships between genes, we examined the effects of knocking out Pax7 and Sox10 on other neural crest transcription factors. To this end, we co-electroporated *CAGG>nls-Cas9-nls*, *CAGG>H2B-RFP*, and control *U6.3>Control.gRNAf+e* on the left side with Pax7-targeting *U6.3>Pax7.1.gRNAf+e* or Sox10-targeting *U6.3>Sox10.1.gRNAf+e* on the right side of gastrulating stage HH4 embryos. The embryos were cultured ex ovo until stage HH9-10 and then processed for *in situ* hybridization for Pax7, FoxD3, Ets1, and Sox10 (Figure 4A). Pax7 knockout resulted in reduced staining for Pax7, FoxD3, Ets1 and Sox10 transcripts in the migratory neural crest (Figure 4B–E). On the other hand, knock-out of Sox10 caused a loss of its own expression, but as expected had no effect on Pax7, FoxD3 or Ets1 (Figure 4F–I), all of which are expressed prior to Sox10 and upstream in the neural crest GRN. Thus, these results recapitulate previously demonstrated gene regulatory interactions (Simões-Costa and Bronner, 2015) and confirm that Pax7 acts as an upstream regulator of FoxD3, Ets1 and Sox10 whereas Sox10 expression is downstream of these transcription factors and its subsequent loss does not affect expression of its upstream regulators.

To further test the ability of CRISPR/Cas9 to decipher direct gene regulatory interactions, we examined the effects of Pax7 loss on one of its direct transcriptional targets, FoxD3. We have previously shown that Pax7 directly regulates activity of FoxD3 at cranial levels by binding to the NC1 enhancer element upstream of the FoxD3 coding sequence (Simões-Costa et al., 2012) (Figure 5A). To confirm this epistatic relationship, we asked if knocking out Pax7 using CRISPR/Cas9 would reduce exogenous FoxD3 NC1 enhancer activity. To this end, we co-electroporated *CAGG>nls-Cas9-nls*, *U6.3>Pax7.1.gRNAf+e*, and *FoxD3-NC1.1>eGFP* reporter construct containing a constitutively active version of the *FoxD3-NC1* enhancer on the right side of stage HH4 embryos (Figure 5B). The left internal control side was co-electroporated with *CAGG>nls-Cas9-nls*, *FoxD3-NC1.1>eGFP*, and *U6.3>Control.gRNAf+e*. After electroporation, embryos were cultured *ex ovo* until stage

HH9-9^{+}. Consistent with the observed Pax7 knockout detected by immunostaining (Figure 5C), the level of eGFP expression was reduced on the side of the embryo that was electroporated with *Pax7.1* gRNA compared to the control side (Figure 5D), validating the requirement of Pax7 for the activation of the FoxD3-NC1 enhancer. While the exogenous reporter activity through the NC1 enhancer was effectively lost, we further hypothesized that the absence of a transcriptional input from Pax7 would result in reduced endogenous FoxD3 protein levels. To test this, we electroporated stage HH4 embryos with *U6.3>Pax7.1.gRNAf+e* and *U6.3>Control.gRNAf+e* on the right and left side respectively, along with *CAGG>nls-Cas9-nls* and *CAGG>H2B-RFP* on both sides, cultures embryos till stage HH9+, and collected cell lysates for immunoblotting. Consistent with our hypothesis, both Pax7 and FoxD3 protein levels were significantly reduced on the side electroporated with the Pax7-targeting gRNA (Figure 5E). Quantification of these data revealed a 4-fold and 15-fold decrease in the levels of Pax7 and FoxD3 protein, respectively (Figure 5F, G) on the side electroporated with the Pax7-targeting gRNA compared to the control side. Taken together, these results demonstrate the applicability of our optimized CRISPR/Cas9 system for investigating direct epistatic relationships among different genes.

The ‘gold standard’ control for demonstrating specificity in loss-of-function experiments is to perform a rescue that recovers function when the lost protein is exogenously supplied. To extend this to our CRISPR/Cas9 system, we asked if we could restore *FoxD3-NC1.1* enhancer activity after Pax7 knockout by over-expressing Pax7 exogenously. To this end, we electroporated the coding sequence of Pax7 under the control of a basal promoter (*CAGG>Pax7CDS-IRES-H2B-RFP* (Roellig et al., 2017)) (Figure 5H) along with *CAGG>nls-Cas9-nls*, *U6.3>Pax7.1.gRNAf+e*, and *FoxD3-NC1.1>eGFP* on the right side of stage HH4 embryos (Figure 5I). The left side was electroporated with *U6.3>Control.gRNAf+e* and served as an internal control. The PAM adjacent to the *Pax7.1* gRNA target site lies in the first intron, and hence would be missing from the Pax7 coding sequence. Since identification of the PAM is essential for Cas9 binding, we predicted that our Pax7 overexpression construct would not be recognized by the Cas9-Pax7.1.gRNA complex. Embryos were developed until stage HH9-10, after which they were imaged for *FoxD3-NC1.1* enhancer driven eGFP reporter expression. The activity of the *FoxD3-NC1.1* enhancer appeared similar on both the control and experimental sides of the embryo (Figure 5J), indicating that exogenous Pax7 rescued the CRISPR/Cas9-mediated loss of endogenous Pax7 protein, and consequently, the *FoxD3-NC1.1* reporter activity, thereby demonstrating specificity. Taken together, these results suggest that our optimized CRISPR system is specific in causing functional gene knockouts at target loci in the chicken genome and demonstrate the functionality of this approach in ordering gene regulatory interactions.

Rapid screening of gRNAs using a Cas9-integrated chicken DF-1 fibroblast cell line

Validating individual gRNAs for knocking out genes *in vivo* using CRISPR/Cas9 can be cumbersome and as a result continues to be one of the potential limitations of designing CRISPR/Cas9 experiments in chick embryos. Although we have reported a simple sorting-based protocol to quantify gRNA efficacy *in vivo*, we sought to develop a simpler strategy to overcome the need for cell sorting. To this end, we have modified the chicken DF-1 fibroblast cell line to constitutively express Cas9 that has been integrated in the genome

using a Tol2-flanked CAGGS-driven *Cas9-2A-Puro*^{R} cassette and *T2TP* transposase (Sato et al., 2007) (Figure 6A). We validated the constitutive nuclear expression of Cas9 by immunostaining using an antibody against Cas9, followed by DAPI-counterstaining (Figure 6B–D). Interestingly, the expression level was variable in different cells, suggesting that the transposase-mediated genomic integration events were distinct. Once we verified the stable integration of Cas9 in DF-1 cells, we used this system to assay the efficacy of gRNAs for *in vivo* application in embryos. To this end, we transfected Cas9-integrated DF-1 cells with gRNAs targeting the genomic loci of genes *Pax7* and *Sox10* using gRNAs described in previous sections (*U6.3>Pax7.1.gRNAf+e* or *U6.3>Sox10.1.gRNAf+e*). As a control for transfection and to calculate the transfection rate, we also transfected a different well of cells with *CAGG>H2B-RFP*. After 48 hours of incubation, we isolated genomic DNA from the Pax7 and Sox10-targeted cells for genotyping. As expected, both gRNAs generated mutations around the gRNA targeting site for the two genes (Figure 6E–F) that would have resulted otherwise in a splicing error and/or frameshift in the coding sequence. Importantly, the efficacy rates for the two gRNAs from unsorted DF-1 cells were consistent with the results obtained from sorted chick embryo cells (Figure 2B, 3B). Taken together, these results demonstrate the utility of our Cas9-DF1 cell line in simplifying the experimental designs for future CRISPR/Cas9 knockout experiments in chick embryos.

Conclusion

In summary, here we demonstrate the application of the CRIPSR/Cas9 system for effective somatic cell genome editing in chicken embryos. The chick embryo offers many advantages for analysis of gene function in amniotes *in vivo* because of its accessibility, ease of manipulation, and low cost. Moreover, the ability to perform bilateral electroporations enables an internal control within a single embryo. In the past, loss-of-function studies have relied upon morpholinos, dominant negatives, or RNAi approaches, all of which are transient, and thus useful for relatively short-term analysis. Although morpholinos offer a rapid and efficient method to block translation or splicing, concerns regarding the possibility of toxicity and off-target effects make it important to consider alternative approaches. To this end, we optimized our Cas9 and gRNA expression plasmids by incorporating three modifications: first, by employing two NLS sequences for higher nuclear expression of Cas9 protein (Chen et al., 2013); second, by using a modified gRNA (“F+E”) scaffold to enhance *in vivo gRNA* transcription (Chen et al., 2013; Stolfi et al., 2014); and third, by using a species-specific chicken U6 promoter. In addition, we have generated a Cas9-DF1 cell line that greatly streamlines the process of gRNA design for knockout experiments in chick embryos. The results highlight the robustness and reproducibility of this modified CRISPR/Cas9 system for generating loss-of-function in chick embryos in a manner that can be applied to many developmental processes, including protein functional analysis and the dissection of gene regulatory interactions.

Materials and Methods

Molecular cloning

The Pax7, Sox10, and Sox2 genomic loci were obtained from the UCSC genome browser (Karolchik et al., 2003). The initial set of gRNA targets were designed by searching these loci for the motif G-<N20>-GG. Protospacer sequences overlapping with splice junctions were preferred over ones within coding sequences. The *Gallus gallus 5.0* genome assembly available on the UCSC genome browser was used to screen for polymorphisms. Using this approach, we generated the gRNA targets used in this study: *Pax7* (GGCCCAGCGGGGTGGACACT), *Sox10* (GAGATCTTGGTCATCAGCCA), and *Sox2* (GCCCAGCAAACTTCGGGGGG). We also designed a control gRNA with a protospacer sequence not found in the chicken genome (GCACTGCTACGATCTACACC). Previously described design principles (Doench et al., 2014; Gandhi et al., 2017; Moreno-Mateos et al., 2015) were followed when choosing between multiple gRNA targets for the same gene to avoid off-target effects. All protospacers were cloned into a modified gRNA "F+E" backbone, which was a gift from Lionel Christiaen (Addgene plasmid # 59986). The human codon-optimized Cas9 was obtained as a gift from Lionel Christiaen (Addgene plasmid # 59987). *nls-Cas9-nls* was PCR amplified using High-Fidelity Phusion polymerase (NEB) and inserted downstream of the chicken beta-actin promoter (*CAGG*). Our gRNA and Cas9 vectors can be obtained through Addgene (https://www.addgene.org/Marianne_Bronner/).

For the U6 promoter optimization assay, the "*gRNA.f+e*" backbone was PCR amplified to remove the terminator sequence from the 3′ end of the scaffold. This amplicon was fused to the 5′ end of GFP using overlap PCR, and this entire cassette was then cloned downstream of the human U6 and chicken U6.3 promoter (gift from Chao-Yuan Yeh at the Cheng-Ming Chuong lab).

For qRT-PCR, following electroporation with the human and chicken U6 promoter constructs, RNA was extracted using the RNAqueous kit (Ambion). cDNA strands were synthesized using SuperScript III Reverse Transcriptase (Invitrogen) using random hexamers, and stored at −20°C. Primers for qRT-PCR against GFP were (for 5′-AAGCTGACCCTGAAGTTCATCTGC-3′, rev 5′-CTTGTAGTTGCCGTCGTCCTTGAA-3′).

Electroporation

Fertilized chicken embryos were obtained from local farmers, and were electroporated at stage HH4 using previously described techniques (Sauka-Spengler and Barembaum, 2008). For Pax7 and Sox10 knockout experiments, the right side of the embryos were electroporated with 2μg/μL *CAGG>nls-Cas9-nls*, 1.5μg/μL *U6.3>Pax7/Sox10gRNAf+e* and 2μg/μL *CAGG>H2B-RFP*, while the left side was electroporated with 1.5μg/μL *U6.3>Control.gRNAf+e* along with Cas9 and H2B-RFP reporter. For the epistasis experiment, 2μg/μL of *FoxD3-NC1.1>eGFP* was electroporated on both sides of the embryo, combined with CRISPR/Cas9 reagents as described above. For overexpression of Pax7, 2μg/μL of *CAGG>Pax7CDS-IRES-H2B-RFP* was electroporated on the right side leaving the other side as control. Electroporated embryos were cultured *ex ovo* in 35mm dishes with

1mL of albumen at 37°C in humidified chambers until the desired Hamburger Hamilton stages were reached (V. Hamburger, 1951).

Genotyping

Whole embryos were electroporated with *CAGG>nls-Cas9-nls* and *CAGG>H2B-RFP* together with either *U6.3>Pax7.1.gRNAf+e* or *U6.3>Sox10.1.gRNAf+e* at stage HH4, then incubated to stage HH10. Live embryos were dissected in Ringer's solution on ice, washed with sterile PBS, and dissociated with Accumax cell dissociation solution (EMD Millipore). Dissociation was terminated by addition of Hanks Buffered Saline Solution (HBSS) (Corning) supplemented with 25mM HEPES pH 7.0, 2.5mg/mL BSA Fraction V (Sigma), and 10mM $MgCl_2$. Cells were then passed through a 40 μm filter to remove debris, and RFP^+ cells were then isolated using a Sony Synergy 3200 cell sorter equipped with a 561nm laser (Caltech Flow Cytometry Facility). Cells were pelleted, then genomic DNA was prepared in 20 μl 1x AccuPrime PCR Buffer II (ThermoFisher). This resuspension was incubated at 95°C for 15 minutes, 2.5 μl 20 mg/ml Proteinase K was added and reincubated at 55°C for 2 hours with frequent pipetting to mix, then heated to 95°C for another 15 minutes. This resulting preparation was used for PCR amplification using AccuPrime High Fidelity Taq Polymerase (ThermoFisher) with Pax7 (for 5′-TAAATCGCGAGGCAATTTCT-3′, rev 5′-GTCCCCTCGACCCTACTTTC-3′) or Sox10 (for 5′-GGAGATATGTGAGCAGACAGG-3′, rev 5′-TTCCATTGACCCGAACAGG-3′) locus primers. Amplicons were then PCR purified (QIAGEN) and TA cloned into pGEM T Easy (Promega) for transformation and Sanger sequencing (Laragen).

In-situ hybridization

Whole mount embryos were fixed in 4% paraformaldehyde for 2 hours at room temperature. Post-fixation, embryos were washed three times in PBS-0.1% Tween, and were serially dehydrated in methanol, after which they were stored at −20°C. *In situ* hybridization for *Sox10* (Betancur et al., 2010), *Pax7* (Basch et al., 2006), *FoxD3* (Kos et al., 2001), and *Ets1* (Barembaum and Bronner, 2013) was performed using previously described protocol (Acloque et al., 2008). *In situ* hybridization for GFP was performed using a modified protocol which involved incubating the embryos in DNase I (Promega) at 37°C for 1 hour (Arede and Tavares, 2008). The DIG-labeled RNA probe against GFP was a gift from Marcos Simões-Costa.

Immunostaining and Imaging

Whole-mount immunostaining was performed using previously described procedures (Ezin et al., 2009). Briefly, embryos cultured *ex ovo* at 37°C post-electroporation were fixed in 4% paraformaldehyde in phosphate buffer for 20 minutes at room temperature. Embryos were then washed three times in PBS-0.1% Triton for 5 minutes each, after which they were blocked for 2 hours at room temperature in 5% donkey serum for Pax7 and Sox10 staining, and 5% goat serum for Pax7 and HNK1 co-staining. Embryos were incubated with primary antibody at 4°C for 1 night for Pax7, and 2 nights for Sox10. The concentrations of primary antibodies used were: Pax7 (1:10; Developmental Studies Hybridoma Bank, Iowa city, Iowa), Sox10 (1:250; R&D Systems Cat # AF2864), HNK1 (1:5; Developmental Studies Hybridoma Bank, Iowa city, Iowa), RFP (1:500; MBL Cat # PM005), GFP (1:500; Abcam

Cat # Ab290), Cas9 (1:500; Diagenode Cat # C15200216). The signal was detected using secondary antibodies Donkey anti-mouse IgG1 Alexa Fluor 488 and Goat anti-mouse IgG1 Alexa Fluor 488 (for Pax7 and Cas9), Donkey anti-goat IgG1 Alexa Fluor 488 (for Sox10), Goat anti-mouse IgM Alexa Fluor 350 (for HNK1), donkey anti-rabbit IgG1 Alexa Fluor 594 (for RFP), and donkey anti-rabbit IgG1 Alexa Fluor 488 (for GFP), respectively, all diluted to 1:500 final concentrations in PBS-0.5% Triton with 5% donkey or goat serum. For DAPI staining, transverse sections were incubated with DAPI (0.1μg/mL) for 5 minutes. Whole mount embryos were imaged on a Zeiss Imager M2 with an ApoTome module. Transverse sections were imaged on Zeiss 710 inverted confocal microscope at the Caltech Biological Imaging Facility. All images were processed using FIJI imaging software (Schindelin et al., 2012).

Cryosectioning

Whole mount embryos immunostained for Pax7 and RFP were incubated in 5% sucrose for 2 hours at room temperature, followed by overnight incubation in 15% sucrose. The next day, embryos were incubated in gelatin at 37°C for 6 hours and then mounted in silicone molds before they were frozen in liquid nitrogen and stored at −80°C until sectioning. 12um wide sections were obtained, incubated in PBS for 30 minutes at 37°C to remove gelatin, and processed for imaging.

Western Blots

Stage HH4 gastrulating embryos co-electroporated with *CAGG>nls-Cas9-nls* and *CAGG>H2B-RFP* together with *U6.3>Pax7.1.gRNAf+e* (right) and *U6.3>Control.gRNAf+e* (left) were cultured *ex ovo* until stage HH9+, and the cranial region was dissected in Ringer's. Dissected heads were split at the midline to collect both "Control" and "Treatment" halves, which were homogenized in 8M urea/2.5% Sodium Dodecyl Sulphate (SDS). 10μg of total protein from the control and treatment groups was run on a 4–12% polyacrylamide gel (ThermoFisher) and transferred to Nitrocellulose for 1h at 100V at 4°C (Amersham Protran Premium 0.2 NC). The membrane was incubated with primary antibodies against Pax7 (1:50), RFP (1:5000), Cas9 (1:5000), and FoxD3 (Santa Cruz; 1:2000) diluted in 5% BSA/TBS-Tween in a sealed bag overnight at 4°C. The membranes were then incubated in secondary antibodies (KPL; α-Mouse 1:15,000; α-Rabbit 1: 30,000) dissolved in 5% milk/TBS-Tween. The Amersham ECL chemiluminescence reagents were used to develop signal, which was then visualized and captured by X-ray autoradiography. Quantification of the films was performed using FIJI (Schindelin et al., 2012).

Cell culture, transfection, and genotyping

Immortalized chicken DF-1 fibroblast cells (ATCC CRL-12203) were cultured at 37°C in 5% CO_2 in DMEM (Corning) supplemented with 10% fetal bovine serum (Gibco) and penicillin/streptomycin (Corning). To generate the Cas9-DF1 cell line, *Cas9-2A-Puro*^{R} was cloned into *pT2K-CAGGS* (Sato et al., 2007) using Gibson Assembly (NEB). Cells were transfected in 12-well plates at approximately 80% confluency using Lipofectamine 3000 (Invitrogen). Briefly, each well received 2μL of Lipofectamine 3000 reagent, 0.5μg of *T2K-CAGG>Cas9-2A-Puro*^{R}, and 0.5μg of *CAGG>T2TP* (Sato et al., 2007), and 2 μL P3000 reagent following the manufacturer's instructions. Transfected cells were incubated for 48

hours before the media was changed. At this point, the first round of selection was performed by treating the transfected cells with 4μg/mL puromycin (Alfa Aesar) for 6 days, making sure that the media was changed every 48 hours. Selected cells were then passaged twice in 8 days in media containing 4μg/mL puromycin to ensure propagation of a pure population of Cas9-integrated DF – 1 cells. To test gRNAs, these cells were transfected with 1μg of *U6.3>Pax7.1.gRNAf+e* or 1μg of *U6.3>Sox10.1.gRNAf+e* using Lipofectamine 3000 as described above. To validate our transfection protocol, a separate well was transfected with 1μg of *CAGG>H2B-RFP*. Cells transfected with gRNA plasmids were then reincubated for 48 hours at which point they were washed with sterile PBS, then trypsinized and genomic DNA was harvested following the QIAGEN DNeasy Blood and Tissue kit instructions. Genotyping was performed as described above.

Supplementary Material

Refer to Web version on PubMed Central for supplementary material.

Acknowledgments

We would like to thank Alberto Stolfi from Lionel Christiaen's lab (New York University) and Chao-Yuan Yeh from Cheng-Ming Chuong's lab (University of Southern California) for reagents, Erica Hutchins for technical assistance, Yuwei Li, Meyer Barembaum and the rest of the Bronner lab for valuable discussions on the project, Elena K. Perry for helpful comments on the manuscript, the Caltech Biological Imaging Facility for technical assistance on imaging, and Jamie Tijerina with the Caltech Flow Cytometry Facility for assistance with flow cytometry. This work was partially supported by the National Institutes of Health (NIH) [R01 DE024157 to MEB and F32 HD088022 to MLP] and the Brazilian National Council for Scientific and Technological Development [PDE 207656/2014-2 to FMV].

References

Ablain J, Durand EM, Yang S, Zhou Y, Zon LI, Huang Y, Wei W, Mayhall EA, Traver D, Fletcher CD, et al. A CRISPR/Cas9 Vector System for Tissue-Specific Gene Disruption in Zebrafish. Dev Cell. 2015; 32:756–764. [PubMed: 25752963]

Acloque H, Wilkinson DG, Nieto MA. Chapter 9 In Situ Hybridization Analysis of Chick Embryos in Whole-Mount and Tissue Sections. Methods Cell Biol. 2008; 87:169–185. [PubMed: 18485297]

Alexopoulou AN, Couchman JR, Whiteford JR. The CMV early enhancer/chicken beta actin (CAG) promoter can be used to drive transgene expression during the differentiation of murine embryonic stem cells into vascular progenitors. BMC Cell Biol. 2008; 9:2. [PubMed: 18190688]

Arede N, Tavares AT. Modified whole-mount in situ hybridization protocol for the detection of transgene expression in electroporated chick embryos. PLoS One. 2008; 3

Bai Y, He L, Li P, Xu K, Shao S, Ren C, Liu Z, Wei Z, Zhang Z. Efficient Genome Editing in Chicken DF-1 Cells Using the CRISPR/Cas9 System. G3 Genes, Genomes, Genet. 2016

Barembaum M, Bronner ME. Identification and dissection of a key enhancer mediating cranial neural crest specific expression of transcription factor, Ets-1. Dev Biol. 2013; 382:567–575. [PubMed: 23969311]

Basch ML, Bronner-Fraser M, García-Castro MI. Specification of the neural crest occurs during gastrulation and requires Pax7. Nature. 2006; 441:218–222. [PubMed: 16688176]

Betancur P, Bronner-Fraser M, Sauka-Spengler T. Genomic code for Sox10 activation reveals a key regulatory enhancer for cranial neural crest. Proc Natl Acad Sci U S A. 2010; 107:3570–3575. [PubMed: 20139305]

Betancur P, Sauka-Spengler T, Bronner M. A Sox10 enhancer element common to the otic placode and neural crest is activated by tissue-specific paralogs. Development. 2011; 138:3689–3698. [PubMed: 21775416]

Carney TJ, Dutton KA, Greenhill E, Delfino-Machín M, Dufourcq P, Blader P, Kelsh RN. A direct role for Sox10 in specification of neural crest-derived sensory neurons. Development. 2006; 133:4619–4630. [PubMed: 17065232]

Chen B, Gilbert LA, Cimini BA, Schnitzbauer J, Zhang W, Li GW, Park J, Blackburn EH, Weissman JS, Qi LS, et al. Dynamic imaging of genomic loci in living human cells by an optimized CRISPR/Cas system. Cell. 2013; 155:1479–1491. [PubMed: 24360272]

Cho SW, Kim S, Kim Y, Kweon J, Kim HS, Bae S, Kim JSS. Analysis of off-target effects of CRISPR/Cas-derived RNA-guided endonucleases and nickases. Genome Res. 2014; 24:132–141. [PubMed: 24253446]

Cong L, Ran FA, Cox D, Lin S, Barretto R, Habib N, Hsu PD, Wu X, Jiang W, Marraffini LA, et al. Multiplex Genome Engineering Using CRISPR/Cas System. Science (80-). 2013; 339:819–823.

Corey DR, Abrams JM. Morpholino antisense oligonucleotides: tools for investigating vertebrate development. Genome Biol. 2001; 2:1015.1–1015.3.

Darnell D, Schoenwolf G. The Chick Embryo as a Model System for Analyzing Mechanisms of Development. Dev Biol Protoc SE - 4. 2000; 135:25–29.

Diao Y, Li B, Meng Z, Jung I, Lee AY, Dixon J, Maliskova L, Guan KL, Shen Y, Ren B. A new class of temporarily phenotypic enhancers identified by CRISPR/Cas9-mediated genetic screening. Genome Res. 2016; 26:397–405. [PubMed: 26813977]

Dickinson DJ, Ward JD, Reiner DJ, Goldstein B. Engineering the Caenorhabditis elegans genome using Cas9-triggered homologous recombination. Nat Methods. 2013; 10:1028–1034. [PubMed: 23995389]

Doench JG, Hartenian E, Graham DB, Tothova Z, Hegde M, Smith I, Sullender M, Ebert BL, Xavier RJ, Root DE. Rational design of highly active sgRNAs for CRISPR-Cas9-mediated gene inactivation. Nat Biotechnol. 2014; 32:1262–1267. [PubMed: 25184501]

Doench JG, Fusi N, Sullender M, Hegde M, Vaimberg EW, Donovan KF, Smith I, Tothova Z, Wilen C, Orchard R, et al. Optimized sgRNA design to maximize activity and minimize off-target effects of CRISPR-Cas9. Nat Biotechnol. 2016; 34:1–12. [PubMed: 26744955]

Le Douarin N, Kalcheim C. The Neural Crest. 1982

Eisen JS, Smith JC. Controlling morpholino experiments: don’t stop making antisense. Development. 2008; 135:1735–1743. [PubMed: 18403413]

Ezin AM, Fraser SE, Bronner-Fraser M. Fate map and morphogenesis of presumptive neural crest and dorsal neural tube. Dev Biol. 2009; 330:221–236. [PubMed: 19332051]

Gagnon JA, Valen E, Thyme SB, Huang P, Ahkmetova L, Pauli A, Montague TG, Zimmerman S, Richter C, Schier AF. Efficient mutagenesis by Cas9 protein-mediated oligonucleotide insertion and large-scale assessment of single-guide RNAs. PLoS One. 2014; 9

Gandhi S, Haeussler M, Razy-Krajka F, Christiaen L, Stolfi A. Evaluation and rational design of guide RNAs for efficient CRISPR/Cas9-mediated mutagenesis in Ciona. Dev Biol. 2017; 425:8–20. [PubMed: 28341547]

Gerety SS, Wilkinson DG. Morpholino artifacts provide pitfalls and reveal a novel role for pro-apoptotic genes in hindbrain boundary development. Dev Biol. 2011; 350:279–289. [PubMed: 21145318]

Ghislain J, Desmarquet-Trin-Dinh C, Gilardi-Hebenstreit P, Charnay P, Frain M. Neural crest patterning: autoregulatory and crest-specific elements co-operate for Krox20 transcriptional control. Development. 2003; 130:941–953. [PubMed: 12538520]

Green SA, Simoes-Costa M, Bronner ME. Evolution of vertebrates as viewed from the crest. Nature. 2015; 520:474–482. [PubMed: 25903629]

Hamburger V, H HL. A series of normal stages in the development of the chick embryo. Dev Dyn. 1951; 88:49–92.

Han J, Zhang J, Chen L, Shen B, Zhou J, Hu B, Du Y, Tate PH, Huang X, Zhang W. Efficient in vivo deletion of a large imprinted lncRNA by CRISPR/Cas9. RNA Biol. 2014; 11:829–835. [PubMed: 25137067]

Jinek M, Chylinski K, Fonfara I, Hauer M, Doudna JA, Charpentier E. A programmable dual-RNA-guided DNA endonuclease in adaptive bacterial immunity. Science. 2012; 337:816–821. [PubMed: 22745249]

Jinek M, East A, Cheng A, Lin S, Ma E, Doudna J. RNA-programmed genome editing in human cells. Elife. 2013; 2013:e00471.

Karolchik D, Baertsch R, Diekhans M, Furey TS, Hinrichs A, Lu YT, Roskin KM, Schwartz M, Sugnet CW, Thomas DJ, et al. The UCSC Genome Browser Database. Nucleic Acids Res. 2003; 31:51–54. [PubMed: 12519945]

Kok FO, Shin M, Ni CW, Gupta A, Grosse AS, van Impel A, Kirchmaier BC, Peterson-Maduro J, Kourkoulis G, Male I, et al. Reverse Genetic Screening Reveals Poor Correlation between Morpholino-Induced and Mutant Phenotypes in Zebrafish. Dev Cell. 2015; 32:97–108. [PubMed: 25533206]

Korkmaz G, Lopes R, Ugalde AP, Nevedomskaya E, Han R, Myacheva K, Zwart W, Elkon R, Agami R. Functional genetic screens for enhancer elements in the human genome using CRISPR-Cas9. Nat Biotechnol. 2016; 34:1–10. [PubMed: 26744955]

Kos R, Reedy MV, Johnson RL, Erickson CA. The winged-helix transcription factor FoxD3 is important for establishing the neural crest lineage and repressing melanogenesis in avian embryos. Development. 2001; 128

Kudo T, Sutou S. Usage of putative chicken U6 promoters for vector-based RNA interference. J Reprod Dev. 2005; 51:411–417. [PubMed: 15812142]

Labosky PA, Kaestner KH. The winged helix transcription factor Hfh2 is expressed in neural crest and spinal cord during mouse development. Mech Dev. 1998; 76:185–190. [PubMed: 9767163]

Lopes R, Korkmaz G, Agami R. Applying CRISPR-Cas9 tools to identify and characterize transcriptional enhancers. Nat Rev Mol Cell Biol. 2016; 17:597–604. [PubMed: 27381243]

Losson R, Lacroute F. Interference of nonsense mutations with eukaryotic messenger RNA stability. Proc Natl Acad Sci U S A. 1979; 76:5134–5137. [PubMed: 388431]

Mali P, Yang L, Esvelt KM, Aach J, Guell M, DiCarlo JE, Norville JE, Church GM. RNA-guided human genome engineering via Cas9. Science. 2013; 339:823–826. [PubMed: 23287722]

Moreno-Mateos MA, Vejnar CE, Beaudoin J, Fernandez JP, Mis EK, Khokha MK, Giraldez AJ. CRISPRscan: designing highly efficient sgRNAs for CRISPR-Cas9 targeting in vivo. Nat Methods. 2015; 12:982–988. [PubMed: 26322839]

Nishiyama A, Fujiwara S. RNA interference by expressing short hairpin RNA in the Ciona intestinalis embryo. Dev Growth Differ. 2008; 50:521–529. [PubMed: 18510713]

Oishi I, Yoshii K, Miyahara D, Kagami H, Tagami T. Targeted mutagenesis in chicken using CRISPR/Cas9 system. Sci Rep. 2016; 6:23980. [PubMed: 27050479]

Orioli A, Pascali C, Quartararo J, Diebel KWKWKW, Praz V, Romascano D, Percudani R, van Dyk LFLFLF, Hernandez N, Teichmann M, et al. Widespread occurrence of non-canonical transcription termination by human RNA polymerase III. Nucleic Acids Res. 2011; 39:5499–5512. [PubMed: 21421562]

Port F, Chen HM, Lee T, Bullock SL. Optimized CRISPR/Cas tools for efficient germline and somatic genome engineering in Drosophila. Proc Natl Acad Sci U S A. 2014; 111:E2967–2976. [PubMed: 25002478]

Qi LS, Larson MH, Gilbert LA, Doudna JA, Weissman JS, Arkin AP, Lim WA. Repurposing CRISPR as an RNA-guided platform for sequence-specific control of gene expression. Cell. 2013; 152:1173–1183. [PubMed: 23452860]

Ren X, Yang Z, Xu J, Sun J, Mao D, Hu Y, Yang SJ, Qiao HH, Wang X, Hu Q, et al. Enhanced Specificity and Efficiency of the CRISPR/Cas9 System with Optimized sgRNA Parameters in Drosophila. Cell Rep. 2014; 9:1151–1162. [PubMed: 25437567]

Roellig D, Tan-Cabugao J, Esaian S, Bronner ME, Kondoh H, Sharpe P, Lovell-Badge R, Stern C, Yan B, Zhang C, et al. Dynamic transcriptional signature and cell fate analysis reveals plasticity of individual neural plate border cells. Elife. 2017; 6:331–342.

Sato Y, Kasai T, Nakagawa S, Tanabe K, Watanabe T, Kawakami K, Takahashi Y. Stable integration and conditional expression of electroporated transgenes in chicken embryos. Dev Biol. 2007; 305:616–624. [PubMed: 17362912]

Sauka-Spengler T, Barembaum M. Chapter 12 Gain- and Loss-of-Function Approaches in the Chick Embryo. Methods Cell Biol. 2008; 87:237–256. [PubMed: 18485300]

Schindelin J, Arganda-Carreras I, Frise E, Kaynig V, Longair M, Pietzsch T, Preibisch S, Rueden C, Saalfeld S, Schmid B, et al. Fiji: an open-source platform for biological-image analysis. Nat Methods. 2012; 9:676–682. [PubMed: 22743772]

Schulte-Merker S, Stainier DYR. Out with the old, in with the new: reassessing morpholino knockdowns in light of genome editing technology. Development. 2014; 141:3103–3104. [PubMed: 25100652]

Simões-Costa M, Bronner ME. Establishing neural crest identity: a gene regulatory recipe. Development. 2015; 142:242–257. [PubMed: 25564621]

Simões-Costa MS, McKeown SJ, Tan-Cabugao J, Sauka-Spengler T, Bronner ME, Sauka-Spengler T, Barembaum M, Betancur P, Bronner-Fraser M, Sauka-Spengler T, et al. Dynamic and Differential Regulation of Stem Cell Factor FoxD3 in the Neural Crest Is Encrypted in the Genome. PLoS Genet. 2012; 8:e1003142. [PubMed: 23284303]

Sternberg SH, Redding S, Jinek M, Greene EC, Doudna JA. DNA interrogation by the CRISPR RNA-guided endonuclease Cas9. Nature. 2014; 507:62–67. [PubMed: 24476820]

Stolfi A, Gandhi S, Salek F, Christiaen L. Tissue-specific genome editing in Ciona embryos by CRISPR/Cas9. Development. 2014; 141:4115–4120. [PubMed: 25336740]

Streit A, Tambalo M, Chen J, Grocott T, Anwar M, Sosinsky A, Stern CD. Experimental approaches for gene regulatory network construction: the chick as a model system. Genesis. 2013; 51:296–310. [PubMed: 23174848]

Thakore PI, M DA, Song L, Safi A, Shivakumar NK, Kabadi AM, Reddy TE, Crawford GE, Gersbach CA, D'Ippolito AM, et al. Highly specific epigenome editing by {CRISPR-Cas9} repressors for silencing of distal regulatory elements. Nat Methods. 2015; 12:1143–1149. [PubMed: 26501517]

Tsai SQ, Zheng Z, Nguyen NT, Liebers M, Topkar VV, Thapar V, Wyvekens N, Khayter C, Iafrate AJ, Le LP, et al. GUIDE-seq enables genome-wide profiling of off-target cleavage by CRISPR-Cas nucleases. Nat Biotechnol. 2015; 33:187–197. [PubMed: 25513782]

Véron N, Qu Z, Kipen PAS, Hirst CE, Marcelle C. CRISPR mediated somatic cell genome engineering in the chicken. Dev Biol. 2015; 407:68–74. [PubMed: 26277216]

Wang T, Wei JJ, Sabatini DM, Lander ES. Genetic screens in human cells using the CRISPR-Cas9 system. Science. 2014; 343:80–84. [PubMed: 24336569]

Wise TG, Schafer DJ, Lambeth LS, Tyack SG, Bruce MP, Moore RJ, Doran TJ. Characterization and Comparison of Chicken U6 Promoters for the Expression of Short Hairpin RNAs. Anim Biotechnol. 2007; 18:153–162. [PubMed: 17612838]

Highlights

- Optimized CRISPR/Cas9 system to target genes in early chick embryos is presented.
- Chick U6 promoter results in increased gRNA transcription compared to human U6.
- CRISPR-mediated knockouts perturb downstream neural crest GRN components.
- Cas9-integrated chicken fibroblast cell line allows for rapid screening of gRNAs.

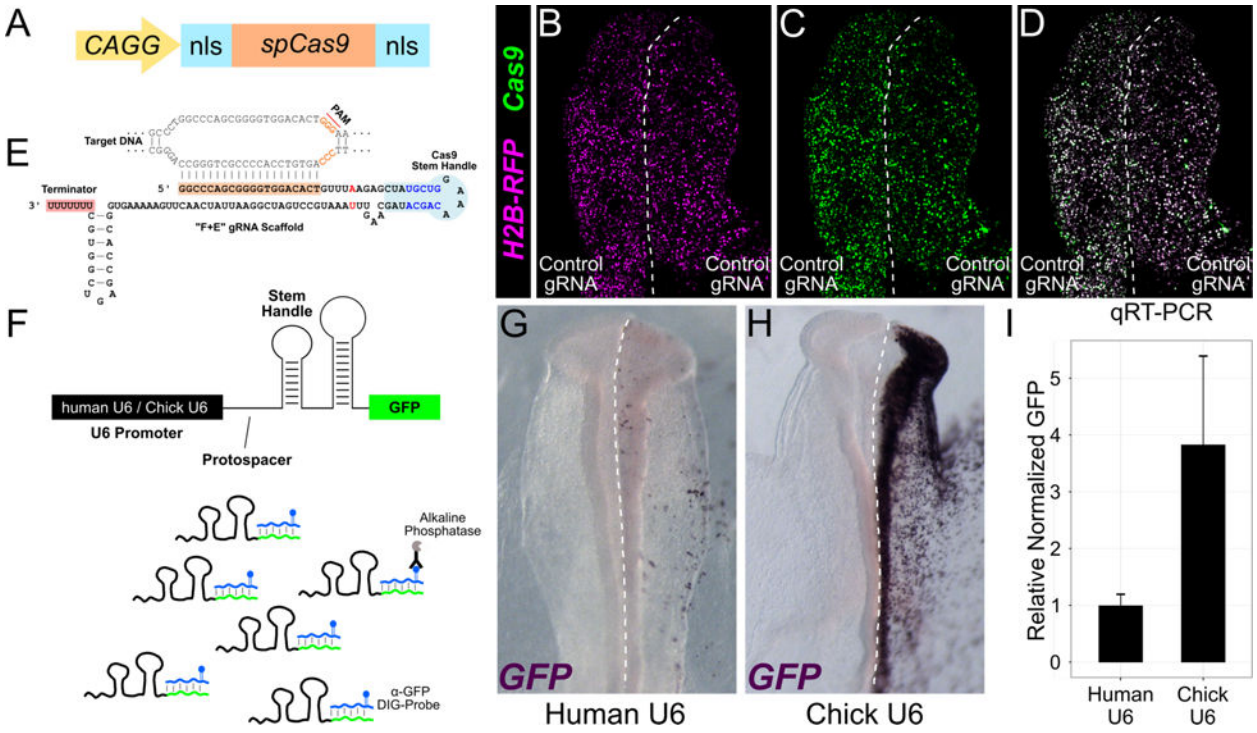

Figure 1. Optimizing individual CRISPR/Cas9 components for application in chick embryos

A. Schematic of the Cas9 construct used in this study. Cas9 flanked with two Nuclear Localization Signal (NLS) sequences was cloned under the regulation of the chicken beta actin promoter (*CAGG*). B–D. Gastrulating Hamburger Hamilton stage HH4 embryos co-electroporated with *CAGG>nls-Cas9-nls*, *U6.3>Control.gRNAf+e*, and *CAGG>H2B-RFP*, cultured *ex ovo* until stage HH9, and immunostained for Cas9 demonstrate efficient nuclear localization of Cas9 protein. Dotted line represents the midline of the neural tube. E. *Pax7.1* protospacer was cloned into a modified "F+E" scaffold. "F" (flip) modification is marked in red, "E" (extension) modification is marked in blue. Watson-Crick base pairing between the protospacer (highlighted in orange) and the target DNA strand is also shown. F. Design for the U6 promoter optimization assay. Human and Chicken U6 promoters were tested for their ability to drive expression of a modified gRNA cassette in which the terminator domain was replaced with GFP (see Materials and Methods for details). Transcripts synthesized through RNA Polymerase III-mediated transcription included the entire GFP sequence, which was then used for qualitative (*in situ* hybridization) and quantitative (qRT-PCR) assessment of promoter efficacy. DIG – Digoxigenin. G–H. Right side of stage HH4 chicken embryos were electroporated with the construct described in F. The embryos were cultured *ex ovo* until stage HH9-10, after which they were fixed and processed for *in situ* hybridization against GFP. The signal obtained in embryos electroporated with the chicken U6 promoter construct (n=3) was stronger than in embryos electroporated with the human U6 promoter construct (n=3). Dotted line represents the midline of the embryo. I. qRT-PCR primers specific to GFP were used to quantify the difference between the human and chicken U6 promoter-driven expression levels. GFP levels were first normalized to housekeeping gene 18S rRNA, and then RFP, which was co-electroporated (*CAGG>H2B-RFP*) along with the construct descried in F to account for electroporation variability between embryos. We observed

nearly a 4-fold increase in the activity of the chicken U6 promoter relative to the human counterpart (n=3 for each group). Error bars represent standard error of the means.

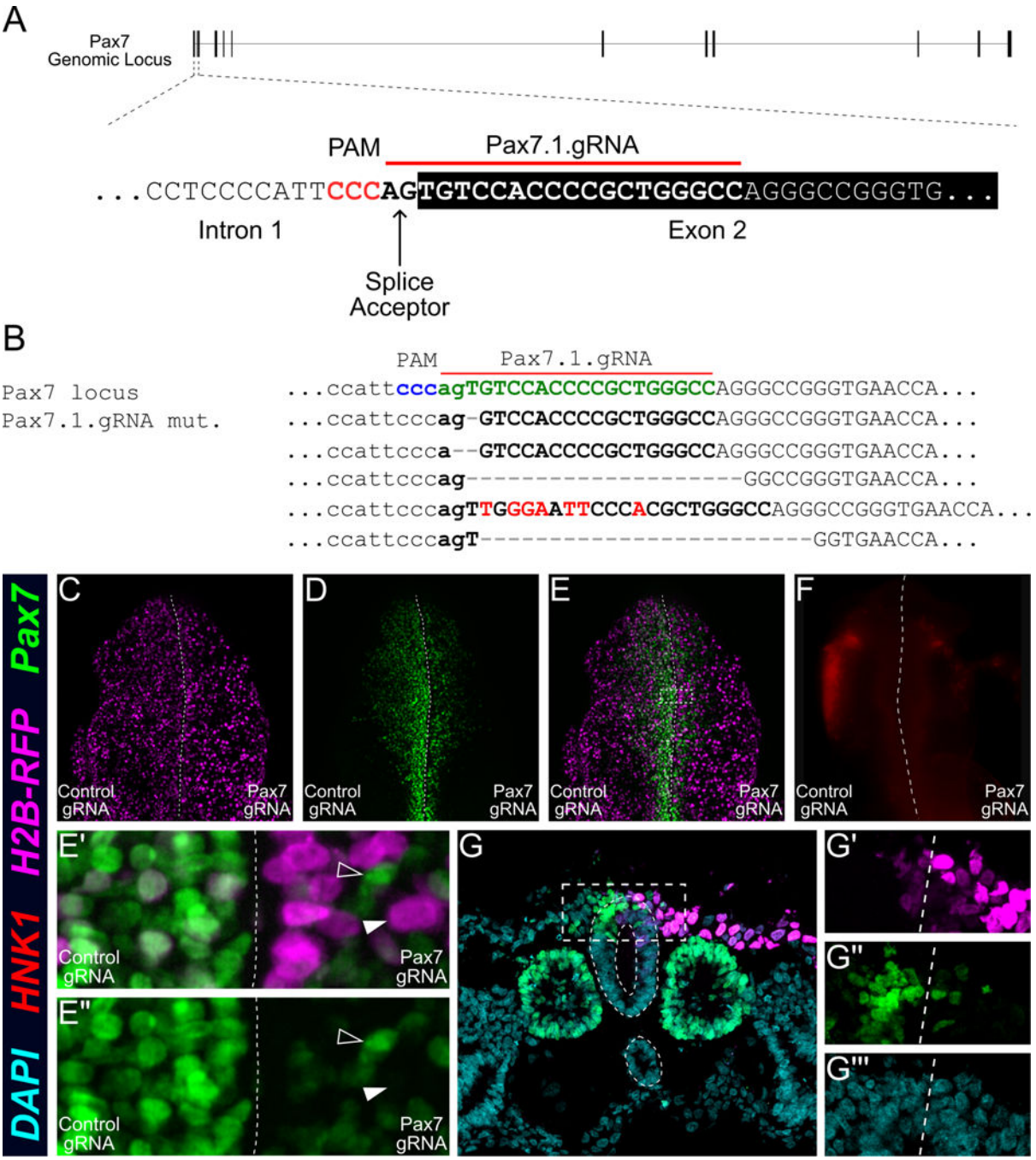

Figure 2. CRISPR/Cas9-mediated knockout of Pax7

A. (Top) The *G. gallus Pax7* gene contains 12 exons (black solid boxes). (Bottom) Nucleotide sequence surrounding the splice junction of exon 2 with the Protospacer Adjacent Motif (PAM) marked in red, and the *Pax7.1.gRNA* protospacer sequence highlighted with a red bar. B. Genotyping of Pax7 knockout cells isolated from HH10 chicken embryos following electroporation of Pax7-targeting CRISPR reagents identifies multiple mutations that would result in a splicing error or frame shift in the predicted protein. C. Stage HH4 embryos were electroporated with *U6.3>Control.gRNAf+e* and

U6.3>Pax7.1.gRNAf+e on the left and right side, respectively, along with *CAGG>nls-Cas9-nls* and *CAGG>H2B-RFP* on both sides, then cultured *ex ovo* until stage HH10. Dotted line represents midline of the neural tube. D. CRISPR/Cas9-mediated knockout of *Pax7* resulted in a dramatic decrease in Pax7 protein level as assessed by immunostaining (n=21/21). E. Overlay of RFP (red) and Pax7 (green) channels revealed that all RFP+ (solid arrowhead) cells were Pax7-, indicating that all transfected cells lost Pax7 protein. Conversely, untransfected cells (E′, E″) retained endogenous Pax7 expression (arrowhead), suggesting that the protein levels in transfected cells on the right side of the embryo were lost as a result of CRISPR/Cas9-mediated activity. F. Embryos were cultured until stage HH10 and immunostained for migratory neural crest expression of HNK1. HNK1 levels on the Pax7 knockout side were considerably reduced compared to the internal control, consistent with the role of Pax7 upstream of migratory neural crest formation. G. Another stage HH4 embryo unilaterally electroporated with *U6.3>Pax7.1.gRNAf+e*, *CAGG>nls-Cas9-nls* and *CAGG>H2B-RFP* on the right side was cultured *ex ovo* until stage HH9 and stained for RFP and Pax7. Nuclei were labeled using DAPI stain. Transverse sectioning through this embryo revealed a nearly complete loss of Pax7 expression in the neural tube (dotted line). The zoomed-in images of the dorsal neural tube show high transfection rate (RFP^+ cells; G′), loss of Pax7 on the right side ($Pax7^-$ cells; G″), and unaffected nuclear morphology ($DAPI^+$ nuclei, G‴).

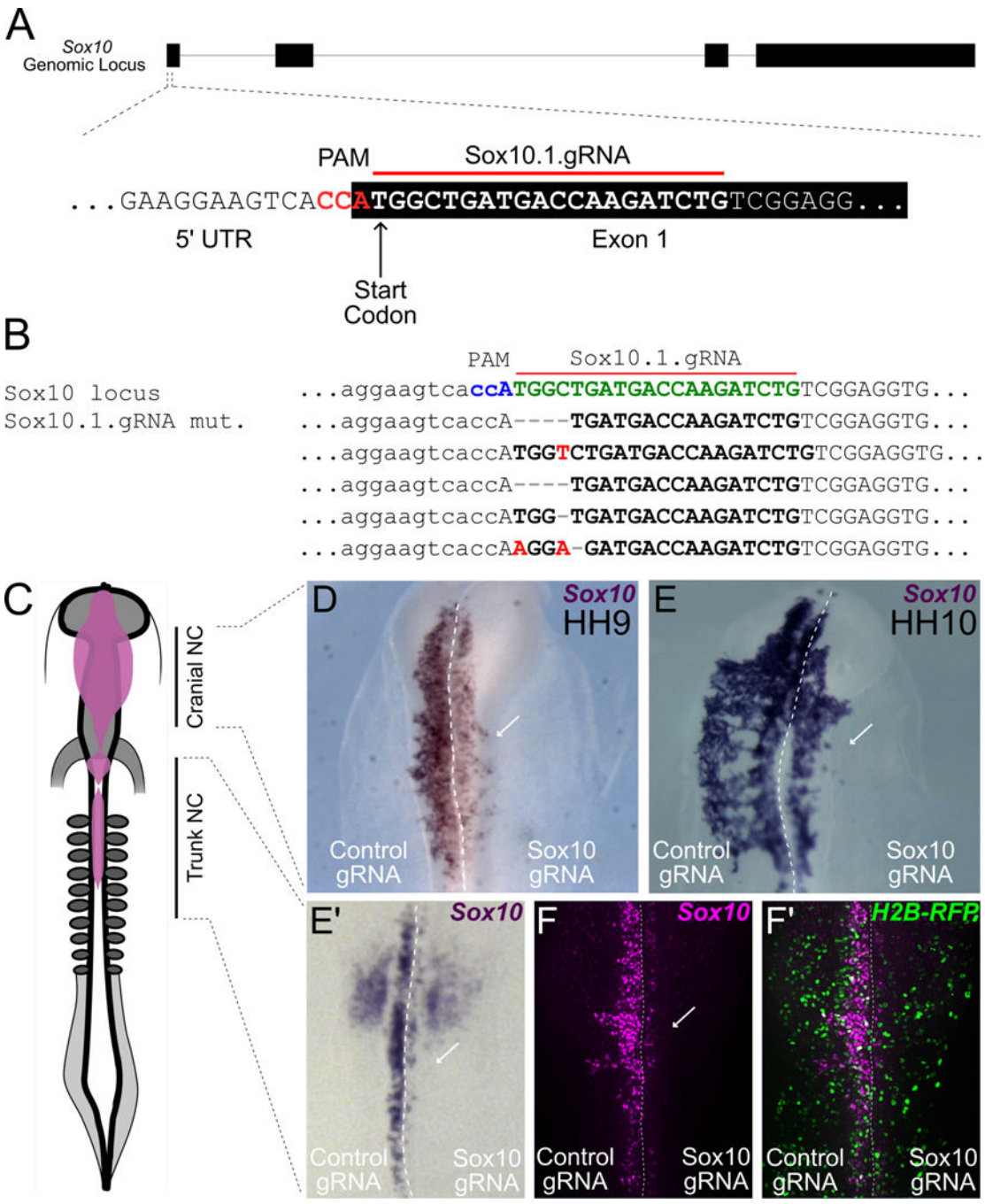

Figure 3. CRISPR/Cas9-mediated knockout of Sox10

A. (Top) Schematic of the *G. gallus Sox10* gene contains 4 exons (black solid boxes). (Bottom) Nucleotide sequence surrounding the Sox10 start codon, with the PAM marked in red, and the *Sox10.1.gRNA* protospacer sequence highlighted with a red bar. B. Genotyping of Sox10 knockout cells isolated from HH10 chicken embryos following electroporation of Sox10-targeting CRISPR reagents identifies multiple mutations that would result in a splicing error or frame shift in the predicted protein. C. A cartoon model of a stage HH10 chicken embryo with the Sox10- expressed migratory cranial and vagal neural crest

(highlighted in violet). Stage HH4 embryos were electroporated with *U6.3>Control.gRNAf+e* and *U6.3>Sox10.1.gRNAf+e* on the left and right side, respectively, along with *CAGG>nls-Cas9-nls* and *CAGG>H2B-RFP* on both sides, then cultured *ex ovo* until stage HH9-10, after which they were processed for *in situ* hybridization against Sox10. D–E. Reduced Sox10 expression levels were observed at stage HH9 in the emigrating cranial neural crest cells (D) and at stage HH10 in the migratory cranial neural crest cells (E). E′. Expression of Sox10 (embryo described in E) was reduced in the vagal neural crest and in the otic placode. Notably, the right side shows a nearly complete loss of Sox10 expression in the neural crest. F. Another stage HH4 embryo electroporated with *U6.3>Control.gRNAf+e* and *U6.3>Sox10.1.gRNAf+e* on the left and right side, respectively, along with *CAGG>nls-Cas9-nls* and *CAGG>H2B-RFP* on both sides, was cultured *ex ovo* until stage HH10, and then immunostained for Sox10 and RFP. The right side shows a nearly complete loss of Sox10 protein compared to the left side control (n=9/9), indicating that CRISPR/Cas9-mediated mutations at the Sox10 locus affected both transcript and protein levels. F′. Expression of Sox10 is detected in RFP^+ transfected neural crest cells on the control side, whereas the transfected cells on the right side are $Sox10^-$.

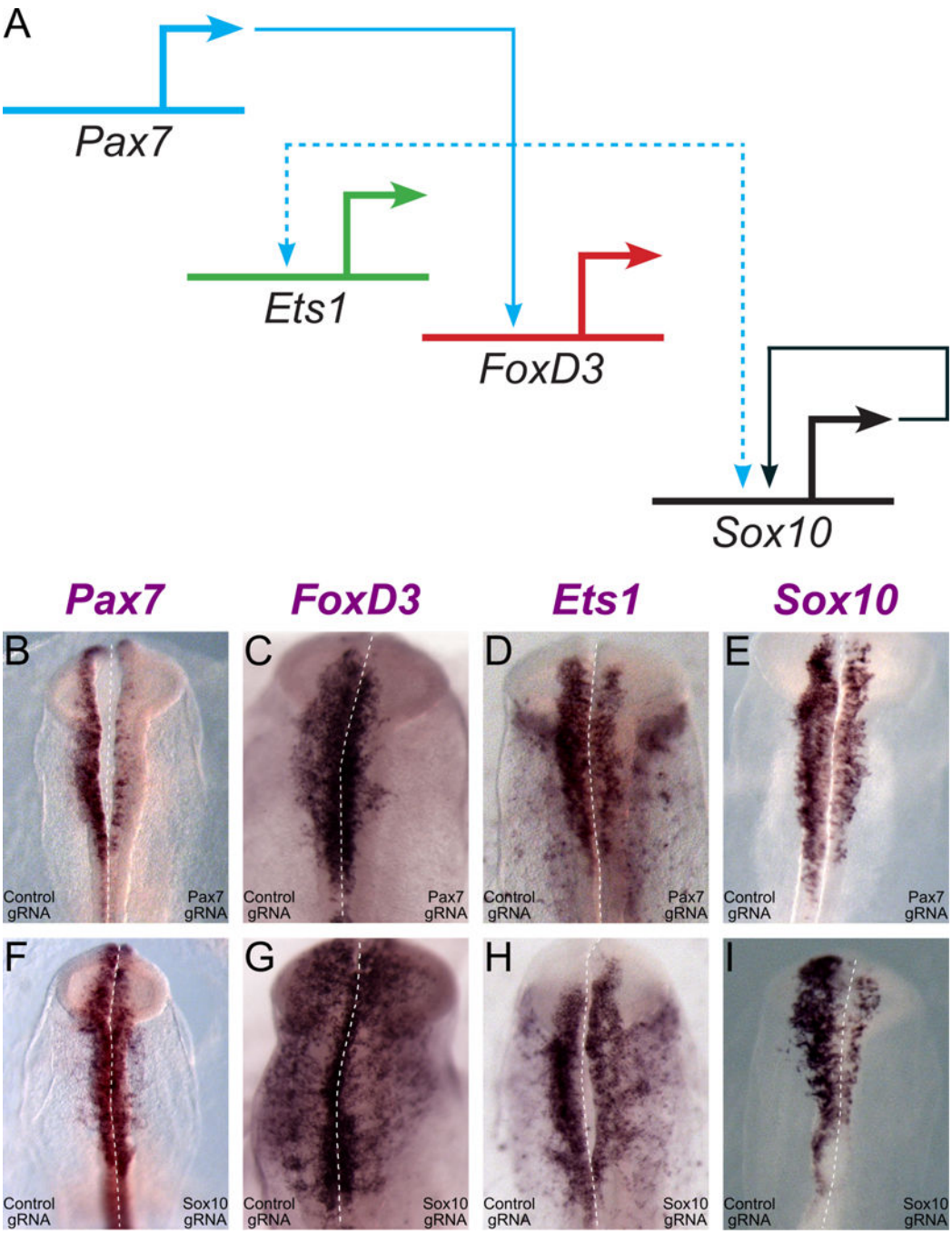

Figure 4. Application of CRISPR/Cas9 to study epistatic relationships

A. Gene regulatory network model derived from previously studies shows regulatory interactions between key neural crest transcription factors. B–E. Gastrulating embryos were electroporated with *CAGG>nls-Cas9-nls*, *CAGG>H2B-RFP*, *U6.3>Control.gRNAf+e* on the left and either *U6.3>Pax7.1.gRNAf+e* (B-E) or *U6.3>Sox10.1gRNAf+e* (F–I) on the right side, cultured until stage HH9-10, then processed for *in situ* hybridization for Pax7 (B, F), FoxD3 (C, G), Ets1 (D, H), and Sox10 (E, I). Pax7 loss resulted in reduced expression of

each downstream target in the neural crest (B–E), while Sox10 loss had no effect on the expression of its upstream regulators (F–I).

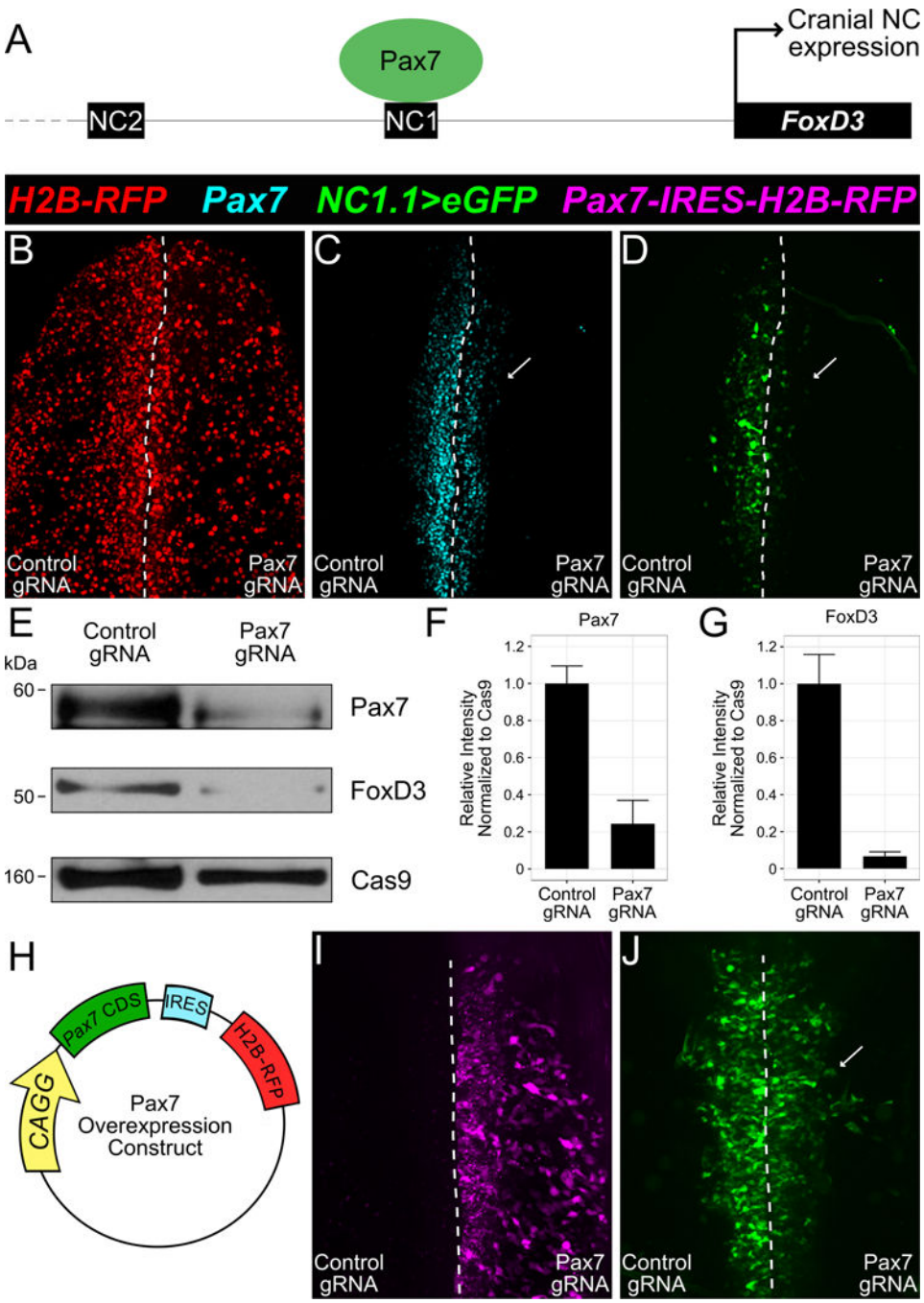

Figure 5. CRISPR/Cas9 allows investigation of direct gene regulatory interactions

A. Pax7 regulates the expression of FoxD3 by direct transcriptional input into the NC1 enhancer. The expression pattern in cranial neural crest cells is reproduced by strong expression from the mutated *FoxD3-NC1.1* enhancer. B–D. Stage HH4 embryos were co-electroporated with *U6.3>Control.gRNAf+e* and *U6.3>Pax7.1.gRNAf+e* on the left and right side, respectively, along with *CAGG>nls-Cas9-nls, FoxD3-NC1.1>GFP*, and *CAGG>H2B-RFP* on both sides. Embryos were cultured *ex ovo* until stage HH9-9^{+}, and reduced Pax7 level was verified using immunostaining (C). The *FoxD3-NC1.1* enhancer

driven expression of eGFP was almost completely lost on the side that was electroporated with *U6.3>Pax7.1.gRNAf+e* (D, arrow), recapitulating the previously published epistatic relationship between Pax7 and FoxD3. E. Embryos electroporated with *U6.3>Pax7.1.gRNAf+e* or *U6.3>Control.gRNAf+e* along with *CAGG>nls-Cas9-nls* were cultured until stage HH9+, after which they were dissected along the midline. Whole cell lysates were isolated from the two groups, and immunoblots were performed using antibodies against Pax7, FoxD3, and Cas9. F–G. Quantitative western blot analysis normalized to Cas9 demonstrates efficient reduction in Pax7 and FoxD3 protein levels following Pax7 knockout when compared to control reagents. Error bars represent standard error of the means (n=3 technical replicates). H–J. To validate the specificity of our optimized CRISPR/Cas9 system, we overexpressed Pax7 using *CAGG>Pax7CDS-IRES-H2B-RFP* (H), and co-electroporated this construct with *CAGG>nls-Cas9-nls, U6.3>Pax7.1.gRNAf+e*, and *FoxD3-NC1.1>GFP* reporter on the right side of a stage HH4 embryo (I–J). The left side was electroporated with *CAGG>nls-Cas9-nls, U6.3>Control.gRNAf+e*, and *FoxD3-NC1.1>GFP*, along with a *CAGG>H2B-RFP* construct. Overexpression of Pax7 rescued the activity of the *FoxD3-NC1.1* enhancer (J), demonstrating the specificity of Pax7 knockout mediated by our optimized CRISPR/Cas9 system.

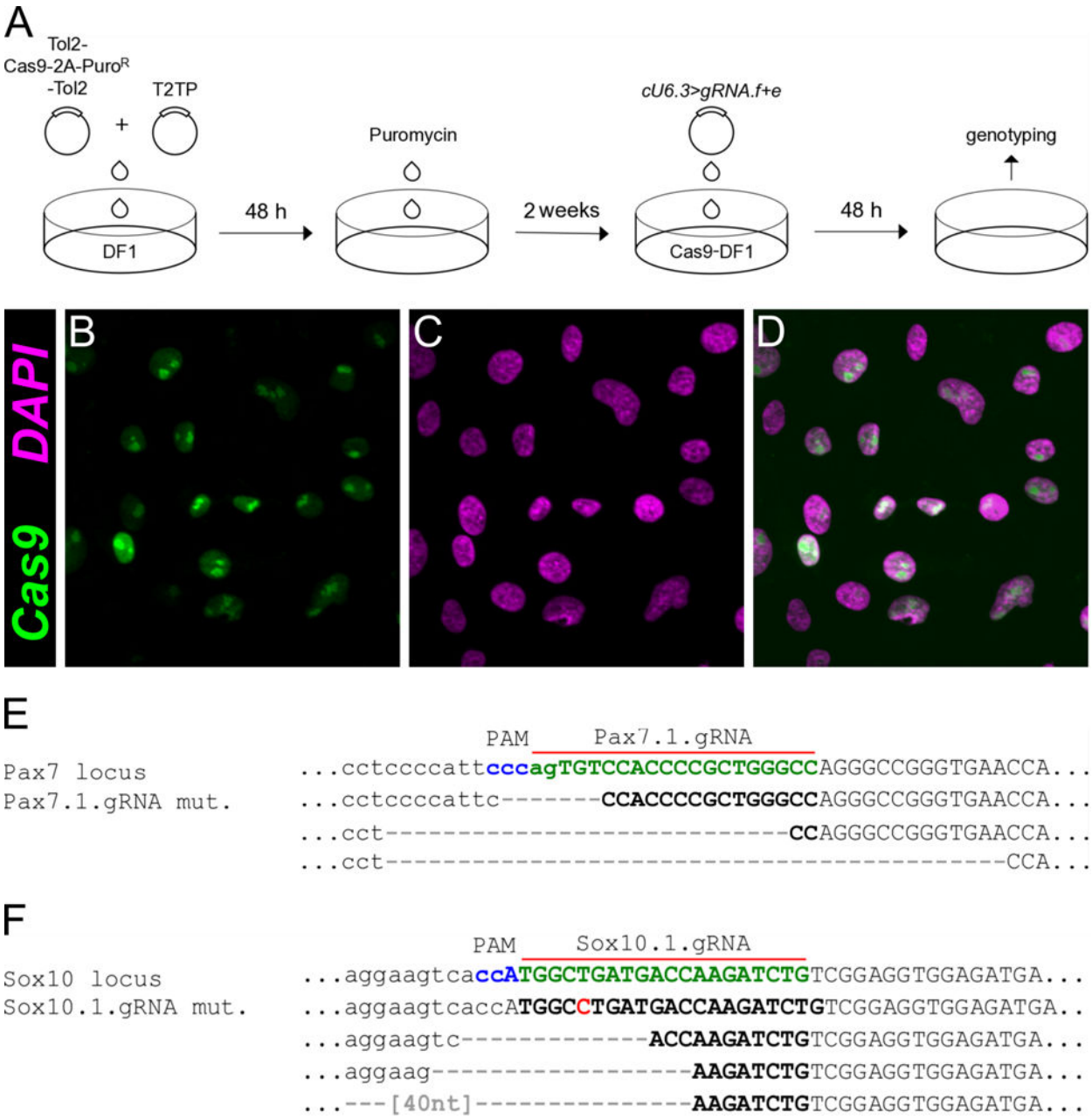

Figure 6. Construction of a Cas9-DF1 fibroblast cell line to validate gRNAs

A. The strategy employed to stably integrate a *Cas9-2A-Puro*^{R} in chicken DF-1 fibroblasts using a T2TP transposase to access gRNA efficacy for *in vivo* applications. Cells were transfected with the two constructs and grown for 48 hours before the first round of selection on puromycin. gRNA plasmids were transfected using a simple lipofectamine-based protocol. B–D. After puromycin selection, the cells were immunostained for Cas9 to validate its stable integration and constitutive expression in the cells. Overlay of Cas9 (green) expression with DAPI (magenta) revealed its proper nuclear localization in the cell line. E–F. Genotyping of Cas9-DF1 cells following transfection with Pax7 (E) and Sox10 (F)

targeting gRNA plasmids identifies multiple mutations that would result in a splicing error or frame shift in the predicted protein *in vivo*.